A Mathematical Model of an Angiogenic Process

Josep Ferre Torres*
Facultat de Fisica, Universitat de Barcelona, Diagonal 645, 08028 Barcelona, Spain.

Advisor: Aurora Hernandez-Machado

Tubular growth of blood vessels in 2-dimensional space is described in the present study by using a phase field model. In contrast with previous studies, we propose a biomechanical model based on Canham-Helfrich energy, coupled to an angiogenic agent through a spontaneous curvature term. The concentration of this angiogenic agent is static and non uniform, generating a well-defined gradient through time. The model is very compact consisting of only one partial differential equation, and has the clear advantage of a reduced number of parameters. Following a phase-field methodology, this model allows us to relate sprout growth with the spontaneous curvature term from the Canham-Helfrich model. The importance of the capillary shape at the initial conditions has also been addressed. Additionally, capillaries grown on other growing capillaries have been obtained by combining multiple distributions of growth factor.

Index terms - Modeling, Simulation and Nanoscopic Methods: angiogenesis, biomechanical modeling, capillary growth, computational modeling, mathematical modeling

I. INTRODUCTION

Angiogenesis is the growth of new capillaries from a pre-existing blood vessel network. This is a complex process usually triggered by cells whose oxygen or nutrient requirements are not satisfied by the current vasculature. New capillaries are generated via sprouting in order to deliver additional nutrients to a growing, injured, or inflamed tissue [1]. The stimulation of angiogenesis can be therapeutic in the case ischemic heart disease or in the wound healing scenario [2]. On the other hand, the inhibition of angiogenesis can be therapeutic in the cases of rheumatoid arthritis and cancer. Notably, angiogenesis plays a pivotal role in tumour development because tumours have the ability to recruit new blood vessels by stimulating vascular growth. Angiogenesis allows tumours to get connected to the circulatory system, receive nutrients, grow beyond a certain size and become malignant when colonizing distant organs [3].

Regarding tumour angiogenesis, the idea that the successful establishment of a solid tumour depends on the formation of new vascularisation has led to the development of many anti-cancer therapies in the past. Most of them were conceived to inhibit the tumour vasculature in order to deprive it from nutrients [5]. Evidence has shown that anti-angiogenic factors, when applied in combination with cytotoxic therapies (i.e. chemotherapy and radiation), are able to enhance treatment efficacy [6]. During the early stages of tumour development, growth occurs through cell division and proliferation. Subsequently, it halts as a result of a lack of nutrients and even develops a necrotic core. Finally, its ability to continue growing relies on the development of a vascular network around the tumour. In this scenario, angiogenesis is responsible for turning a benign tumour into a malignant one, which will

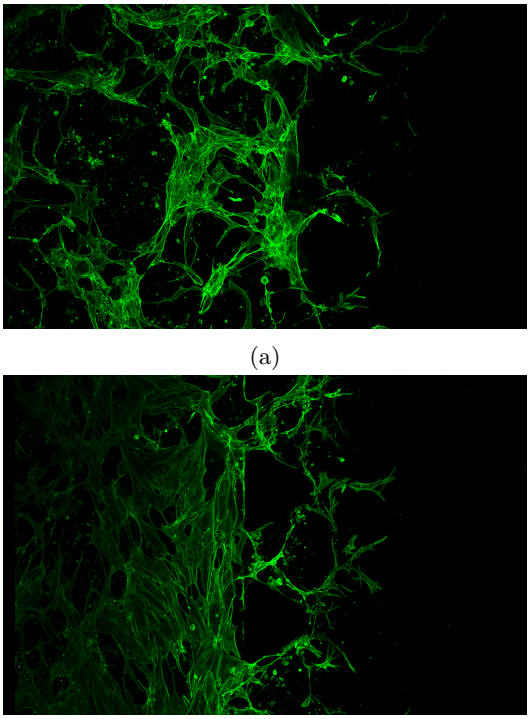

(a)

(b)

Figura 1: Images of endothelial cell cultures after 2 days of growth. Panel (a) illustrates angiogenic phenomena in the absence of stimulating angiogenic agents. Panel (b) shows an endothelial cell culture to which a stable gradient of growth factor has been applied. Images taken from Adrian Lopez Ph.D. thesis [4]

* Electronic address: jferreto10.alumnes@ub.edu

possibly metastasize to other parts of the body, often leading to morbid and mortal consequences for the patient. Tumours give rise to dense and altered capillary networks, which are significantly different from those formed in physiological conditions (see in Fig.1 (a) from [7]). Arguably, the most characteristic feature of tumour-induced capillaries is that they are angiogenic factor dependent, as has been suggested by numerous studies [8–10].

To improve our understanding of the basic mechanisms underlying angiogenesis, both in vitro experiments and mathematical simulations have been carried out over the past three decades, with mathematical and computational models gradually complementing experimental approaches [11]. The use of high resolution microscopy has given rise to the possibility of qualitatively monitoring the progression of vasculature, which has allowed for the testing of hypotheses that lead to development of mathematical models. In the literature we can basically find two different mathematical models of tumour-induced angiogenesis: microscopic descriptions for cell dynamics [12–15] and coarse-grained descriptions based on a diffusive interface [15–17]. The study of the formation of a vascular network requires a unified approach that puts together both, phenomena at the cellular level and large-scale, collective movements of the cells in response to endothelial cell proliferation [18, 19].

In the angiogenesis problem, we are interested on the interfacial effects between two phases that drive the dynamics of the system. Traditional methods, to deal with this kind of problems, need to track the position of the interface at each time in order to solve the dynamics of the system. They solve the coupled problem of the bulk and the moving boundary from different dynamic equations. To avoid this computational limiting step, we aim for the so called phase-field models to write a dynamic evolution for a field (i.e. the phase-field) without any need to explicitly supply information on the interface position. We model the system as a whole.

The phase field theory has shown in previous studies to be very efficient to solve problems where the interfacial effects are driving the dynamics of the system. Phase field theory has been used to model angiogenesis due to the combination of the benefits of a continuum physics to resolve capillaries at a full scale and to represent their structure [19–21]. Furthermore, because it is not computationally expensive, such theory does not only capture the long-term dynamics of angiogenesis, but can also be coupled with tumour growth models or different fluid dynamics simulations [7, 22].

The present project aims at giving further insigths into the basic mechanisms of the angiogenic process by using a biomechanical model. This biomechanical model has never been used for this purpose, to describe the capillary growth problem. The model that we are here implementing is based on the Canham-Helfrich bending energy. We asses the efficacy of the phase-field model and prove that it can be used for growing capillaries. Applying it to this growth mechanism, we pretend to introduce a new tool for future quantitative measurements and predictions via numerical simulations. In this work we consider concepts, such as spontaneous curvature, from the mentioned model that should be extrapolated to the field of angiogenesis.

II. MATHEMATICAL MODEL

Modelling sprouting angiogenesis has to take into consideration biological signals as well as relevant physical processes. Any physical parameter describing these mesoscopic phenomena should not be considering internal structure. Indeed, phase-field models are focused on the movement of the boundaries between domains making them suitable to model morphology and growth of biological systems. Phase-field treats this moving interface as a diffuse interface in order to assimilate it to the bulk.

The dynamic equations constituting the phase-field have different plateaux as equilibrium solutions. Each of these plateaux representing a phase. Between phases a smooth transition is found in a tanh-like shape function (see in Fig.2). This region is called the diffuse interface region. In this work, the given value of the order parameter ($\phi = \pm 1$) is defining the capillaries and the extravascular region, whereby the transition between these represents the interface of the capillary wall. According to the basis of the phase-field, the width of the interface of the capillary wall should be negligible, tend to zero when compared with other length scales. The width of the interface is characterized by a small parameter of the model, ϵ, which has to be numerically smaller than all the other length scales in the system [23]. We did not pay much attention of which value of the phase field was representing each phase as our model treats them equivalently but for the anisotropy term. In consequence, when exploring the effects of this anisotropy we decided which value of the phase-field was representing each phase after obtaining the results.

The Canham-Helfrich model, basically writes down a complete energy functional (Hamiltonian) depending on the curvature energy density. This bending energy is related to the curvature by the expression

$$U \sim \int dA \left(\frac{1}{R_1} + \frac{1}{R_2} \right)^2 \tag{1}$$

Where R_1 and R_2 are the two principal curvatures of the surface at a given point. We have modelled this vessel sprouting taking into account the bending energy and introducing asymmetry through the spontaneous curvature C_0. With no preferred curvature, a surface would relax to a state with zero curvature, however here we impose the appearance of a spontaneous curvature on the surface. This spontaneous curvature stands for the chemical and mechanical characteristics of the extra-cellular matrix such as angiogenic factors. In other words, the

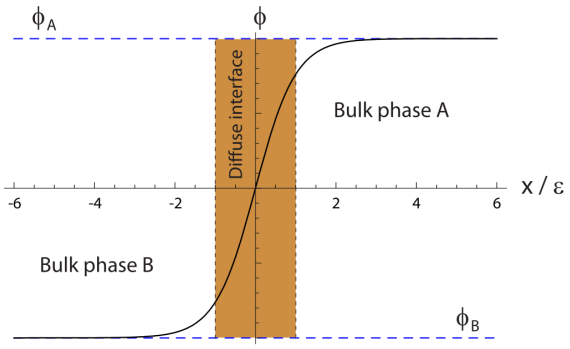

Figura 2: Qualitative profile of a phase-field, $\phi(x)$, in one dimension. The phase-field continuously goes from one phase to the other in a thin but finite region, the diffuse interface (dark region). Figure taken from Felix Campelo Ph.D. thesis, Ref. [24]

spontaneous curvature term can stand for either an angiogenic factor, the extra-cellular matrix structure or any other chemical or mechanical characteristic. Specifying what is the element that generates this anisotropy is not in the scope of this work although we extrapolated it as an angiogenic factor. In the present model, we have considered for simplicity a static and general angiogenic factor even though we acknowledge they can diffuse along the system.

Our system is physically defined by the already existing capillary and the extra-cellular matrix. In this situation, we model this problem of two different phases in two-dimensions. Being a two-dimensional two-phase problem, the phase field, ϕ, has to be a smooth well-behaved function which takes real values in the whole two-dimensional domain, Ω. The phase-field is defined by an expression of the free energy of the system $\mathcal{F} = \int \mathcal{L}\left(\phi, \boldsymbol{\nabla}\phi, \nabla^2\phi\right)$ where $\mathcal{L}$ is the energy density of the system. The free energy, $\mathcal{F}$ is a functional where we add the spontaneous curvature term in order to incorporate the anisotropy,

$$\mathcal{F}_{SC} = \int_{\Omega} \Phi^2_{SC}[\phi] dV, \tag{2}$$

where

$$\Phi_{SC}[\phi] = \Phi[\phi] - \epsilon C_0(\phi^2 - 1)$$

$$\Phi[\phi] = -\phi + \phi^3 - \epsilon^2\nabla^2\phi$$

The term C_0 is related to the spontaneous curvature of ϕ, and the term $(\phi^2 - 1)$ acts as a δ-function centered at the interface, so it confines this effect far from the bulk phases. The interface is consequently forced to accommodate its surface to the spontaneous curvature C_0 which, at the same time, is related with the angiogenic agent. It is important to mention that this phase-field model can be obtained from the formulations of the Canham-Helfrich problem and that both models are equivalent [25]. This spontaneous curvature is position-dependent since we want a non-uniform distribution in the space. So the mechanism of action of the spontaneous curvature term should show different growth-modulatory effects when changed significantly.

Once ϕ and C_0 are defined in the space, we should establish their evolution in time. We have assumed that C_0 is non-time dependant so its distribution will remain constant during the whole process. However, ϕ is subjected to diffusion (Cahn-Hilliard dynamics) but at the same time is locally conserved. If D is the diffusion coefficient for ϕ, its dynamics is governed by

$$\frac{\partial\phi}{\partial t} = \boldsymbol{\nabla}\cdot\left(D\boldsymbol{\nabla}\frac{\delta\mathcal{F}}{\delta\phi}\right) \tag{3}$$

where computing the functional derivative in 3 leads to the final basic dynamic equation for the phase-field that reads as:

$$\frac{\partial\phi}{\partial t} = D\nabla^2\left(\left[3\phi^2 - 1 + 2\epsilon C_0\right]\Phi_{SC}[\phi] - \epsilon^2\nabla^2\Phi_{SC}[\phi]\right) \tag{4}$$

III. METHODS

Our model is simulated numerically by approximate $\phi(x, y, t)$ as a discrete representation on a rectangular grid of points labeled by one index in x and y directions (see in Fig.3). Values of $\phi(x, y, t)$ on this grid are represented on a computer by an array (matrix) of real numbers. The distance between grid points is assumed to represent a small distance Δx in both directions ($\Delta x = \Delta y$ for simplicity). Similarly, time is made discrete by introducing a numerical length scale Δt. We have set an squared grid where the maximum number of grid points in the numerical array to $N = L/\Delta x$, L being chosen as a multiple of Δx.

The numerical integration to advance the solution of Eq.(4) forward in time is known as Euler method. In this method, the solution of ϕ at time $t + \Delta t$ is determined entirely from the solution at time t. We also used a finite-difference method to define the discrete Laplacian by using the five-point stencil finite-difference method [26]. We have designed our domain by introducing periodic boundary conditions on top and bottom limits and Dirichlet boundary conditions on left and right sides of the domain.

When we use a static distribution of the spontaneous curvature term, we are assuming that the diffusion process of the element in the system generating this property is faster than the growth and deformation of the surface. As a consequence of this assumption, we neglect the possible changes of distribution that the angiogenic factor might suffer and use stationary spatial patterns for the spontaneous curvature term. When implementing the model, first of all, we have chosen a static pattern of curvature C_0, which is the anisotropy input for the evolving

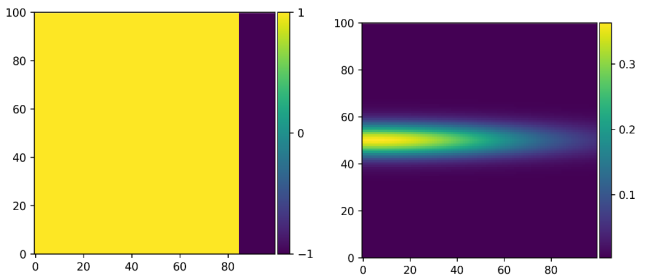

(a) (b)

Figura 3: (a) Initial conditions for the phase-field where $\phi = -1$, on the right side, is representing a single vessel. (b) Representation of the spontaneous curvature term distribution on the domain.

domain ϕ. In most cases, this pattern was a function of a two-dimension Gaussian distribution

$$G(x,y) = A\exp\left\{-\left(\frac{(x-x_0)^2}{2\sigma_X^2} + \frac{(y-y_0)^2}{2\sigma_Y^2}\right)\right\} \quad (5)$$

where the coefficient A is the amplitude, x_0, y_0 is the center and σ_X, σ_Y are the x and y standard deviation respectively. In Tab.I its written the dependence of C_0 with the Gaussian distribution.

In our computations we solved the dynamic evolution with time scale $\Delta t = 10^{-4}$ and grid parameters, N_x and N_y equal to 100. The grid-step Δx and Δy are defined equal to 1. The parameter ϵ characterizing the width of the diffuse interface has been given the same value as the grid-step. As mentioned before, it should have the minimum value possible in the simulation in order to be negligible. These parameters where chosen to reduce the computational time and to accurately simulate the phase-field composed by the bulk-field plus its interface, where $\phi \in (-1, 1)$.

The parameters of the anisotropic term were chosen to study its effect on the simulations. Several amplitude coefficients for the spontaneous curvature term and distinct normal distributions were used to identify its effect on capillary growth. For the application of our model, we defined certain initial conditions, depending on each case. Finally the diffusion coefficient which is related with the speed of the field to react to different stimuli. This coefficient is equivalent to the concept of mobility, M, when applied to the spreading out of cells. It was set for all the simulations equal to one for both phases.

Phase-field computational parameters	
Δx	1
Δt	0.0001
N_x	100
N_y	100
M	1
ϵ	1
C_0	$a \cdot (0{,}1 + G)^2$

Cuadro I: List of the phase-field computational parameters used in capillary growth simulations if not said contrary.

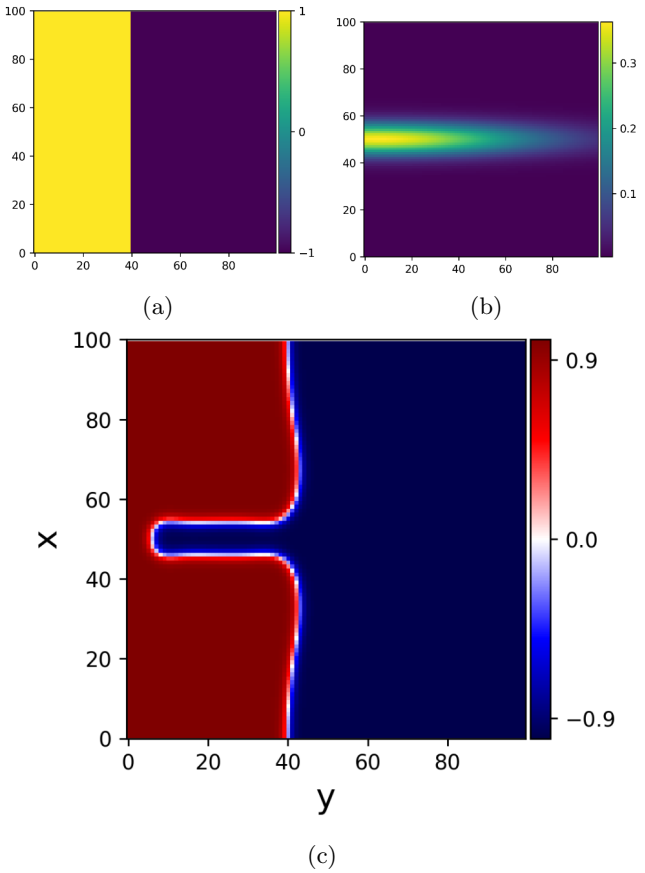

(a) (b)

(c)

Figura 4: Initial domain, spontaneous curvature term distribution and growth pattern. Panel (a) shows the initial domain of a single vessel (phase -1; purple colour). Panel (b) depics the curvature distribution of the spontaneous curvature term in the domain. Panel (c) illustrates the growth pattern of the domain (capillary growth) taken at the time-step $22 \cdot 10^6$.

IV. RESULTS AND DISCUSSION

Starting from a single capillary we are able to grow a new capillary(see in Fig.4). This is activated by the local gradient of the spontaneous curvature term, i.e. the angiogenic factor. The gradient of angiogenic factor leads the growth of the structure towards the source of angiogenic factor.

We set as initial conditions of the domain a thick flat capillary on the right side of the domain, Fig.4(a). The center of the capillary grows from where the distribution of the spontaneous curvature term on the domain changes more abruptly (see in sub-Fig.4(b)). In Fig.4(c) we can see the final state of the tubular growth for the given conditions. This result shows that the tip of the capi-

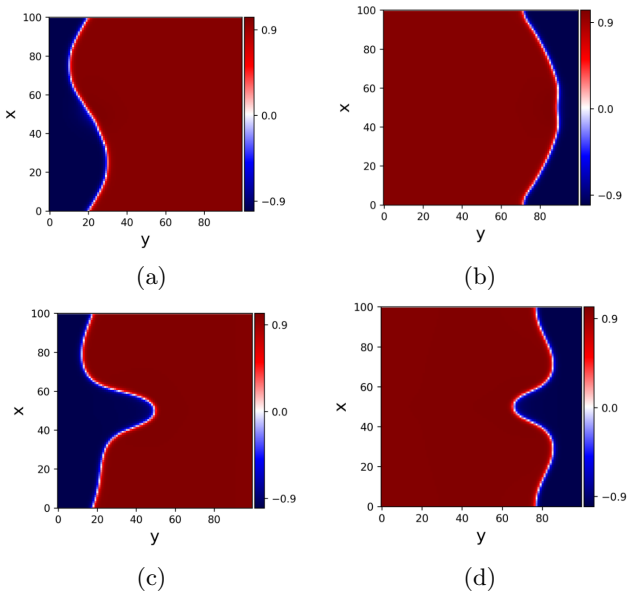

Figura 5: Different initial conditions for the capillary vessel and its growth. Panels (a),(b) illustrate the initial condition, after the interface is formed, of the capillary at the time-step: $20 \cdot 10^3$. (c) and (d) images are taken at time-steps $44750 \cdot 10^3$ and $26200 \cdot 10^3$ respectively.

llary grows in the available region with more pronounced changes in curvature. The initial conditions were not a determinant factor for the evolution of the system. This was proven by generating tubular growth from different conditions (see in Fig.5). The sub-figures from Fig.5 (c) and (d), does not show their equilibrium state because we just wanted to see if the capillary was able to grow in a variety of different initial conditions. The Gauss function used in these simulations was for the sinusoidal-crest-valley system: centered at $y_0 = 90$, $x_0 = 50$, and $\sigma_X = 2$, $\sigma_Y = 0{,}5$. The sinusoidal-valley system had the exactly same Gauss function distribution but centered at $y_0 = 90$. Both of them had defined a curvature amplitude a of 0,5. Additionally, increasing the gradient results in an overall increase of the capillary advancement per unit of time. The smaller the gradient, the slower motion of the capillary which results in slightly wider capillaries.

Moving forward, we tried to grow a capillary from a capillary that was still growing. This simulation was done by with a different angiogenic factor combining two Gaussian distributions for an initial flat capillary as can be seen in Fig.6. The result of this simulation is presented in Fig.7. The initial domain pattern and its Gaussian distribution defining the static spontaneous curvature term in Fig.6. The capillary grows following the maximum change in the spontaneous curvature term. In this case, we had grown the other phase by changing the sign of the coefficient a of the C_0 in Tab.I. The phenomenological behaviour found here has not changed. Therefore proving that our model is able to treat both phases, $\phi = \pm 1$, without difference as stated before. It is noticeable from the

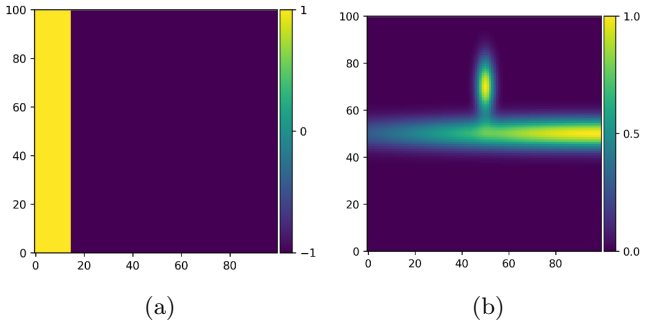

Figura 6: Panel (a) illustrates the initial domain: a single flat capillary on the left side of the domain. Panel (b) shows the Gaussian distribution of the spontaneous curvature term.

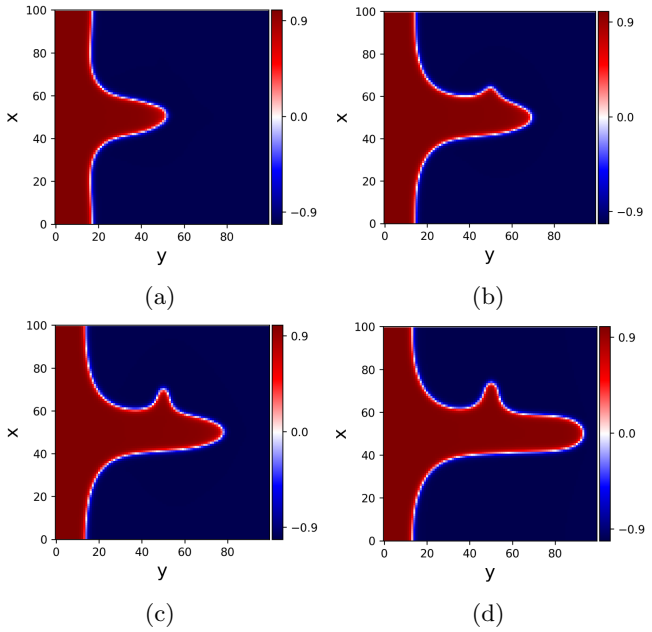

Figura 7: Cactus-like capillary pattern. Time sequence of the emergence of a new capillary from an advancing capillary. Sub-figures (a)-(b)-(c)-(d) are taken at time-steps: $50 \cdot 10^6$, $100 \cdot 10^6$,$120 \cdot 10^6$ and $150 \cdot 10^6$ respectively.

sequence of images shown in Fig.7 that the advancement rate of each tip is different. The phenomenologycal behaviour found here has not changed. Therefore proving that our model is able to treat both phases.

It is remarkable that relatively small variations in magnitude of the parameters that regulate the capillary growth in our model, may lead to different instabilities on the bulk. When introducing more than just one Gaussian distribution of the angiogenic factor better care should be taken in order to have well-defined gradients to avoid extra phenomena, such as double-tip splitting.

We observe how different effective variances, widths, of the Gaussian distribution affect to the width of the

capillary. The wider the spontaneous term distribution the wider the grown capillary. Additionally, if using different amplitude coefficients for the spontaneous curvature term, we do also observe different growth velocities. By comparing sub-Fig.7(b) and sub-Fig.7(d), we see how the smaller capillary growing on the upper direction advances much slower than the bigger capillary growing to the right-side of the domain.

V. CONCLUSIONS AND FUTURE WORK

Based on the phase-field approach we constructed a mathematical model for capillary growth. This biomechanical model is constructed based on Canham-Helfrich bending energy. As a result, the simulated domain evolves according to the minimization of the free energy based on the bending energy of the interface in our system. The term of spontaneous curvature is used here to introduce local anisotropy to our domain, representing the distribution of concentration of angiogenic factor. This anisotropy is what stimulates the growth and advancement of the new capillary. With all this, the model that we presented is capable of simulating sprouting angiogenesis.

The model simulates feasible sprouting capillary as long as we introduce the non uniform spontaneous curvature term. We verified that the growth of the capillary is a local process so it just depends on the local characteristics of the spontaneous curvature term. Moreover, we observed different velocities on the advancement of the capillary. This observation will allow us to make quantitative studies, such as velocity growth rates as a function of the gradient of the spontaneous curvature term in the future. Additionally, surface tension could be introduced to study its relation with growth by measuring the advancement of the capillary when defining different surface tension coefficients. Stability studies of the tubular growth as a function of surface tension, tubular length and width are also from interest.

The validation of this model could be done by realizing a precise characterization of the concentration of a well-known angiogenic factor in an angiogenic process. We suggest using the experimental setup presented in the Ph.D. thesis of Adrian Lopez [4] (see in Appendix A) as it allows to have a well-defined concentration gradients. If validated, the model presented in this work could be used in many more experimental setups to validate and suggest different biological hypothesis. This sort of systematic theory/experimental comparison requires an exhaustive work coming from both sides and will be the aim of a future work.

SUPPORTING INFORMATION

Apéndice A: Experimental setup presented by Ph.D. thesis of Adrian Lopez.

The experimental setup proposed to validate this model is based on PDMS devices obtained from a SU-8 2100 photoresist master following the well-established soft-litography method. The design is based on two neighboring chambers with dimensions: 8415 μm of chamber length, 1300 μm of chamber width and two channels of 500 μm channel width used to generate the gradient of growth factor (see in the Fig.8 for an schematic representation). The chambers are delimited by arrays of microposts, which allow us to confine hydrogels by combining their geometric angle with surface tension phenomena. In their case, the used hydrogel is fibrin, which is obtained by mixing fibrinogen at a concentration of 2.5 mg/mL with thrombin at 1 U/mL. One of the chambers is used to form the endothelial network (1 day of culture) by resuspending HUVECs (Human Umbilical Vein Endothelial Cells) between passages 3 and 8 at a density of $12 \cdot 10^6$ cells/mL in the fibrin gel. The other chamber is just acellular fibrin, and it is used as a space to study angiogenesis. This phenomena is stimulated by creating a stable gradient of growth factors for 2 days by flowing regular media in one channel and media supplemented with VEGF (Vascular Endothelial Growth Factor) at a concentration of 50 ng/mL in the opposing one (both at a rate of 100 μL/h).

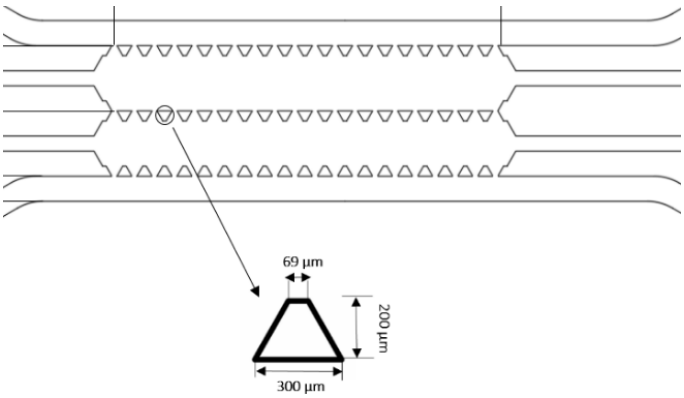

Figura 8: Schematic representation of the experimental setup for the validation of the biomechanical model currently presented. Figure taken from Adrian Lopez Ph.D. thesis[4].

Acknowledgments
We are grateful to Fernández A. and Hernandez-Machado A. for useful and fruitful discussions. We are also indebted to Lopez A. for kindly providing us his experimental results.

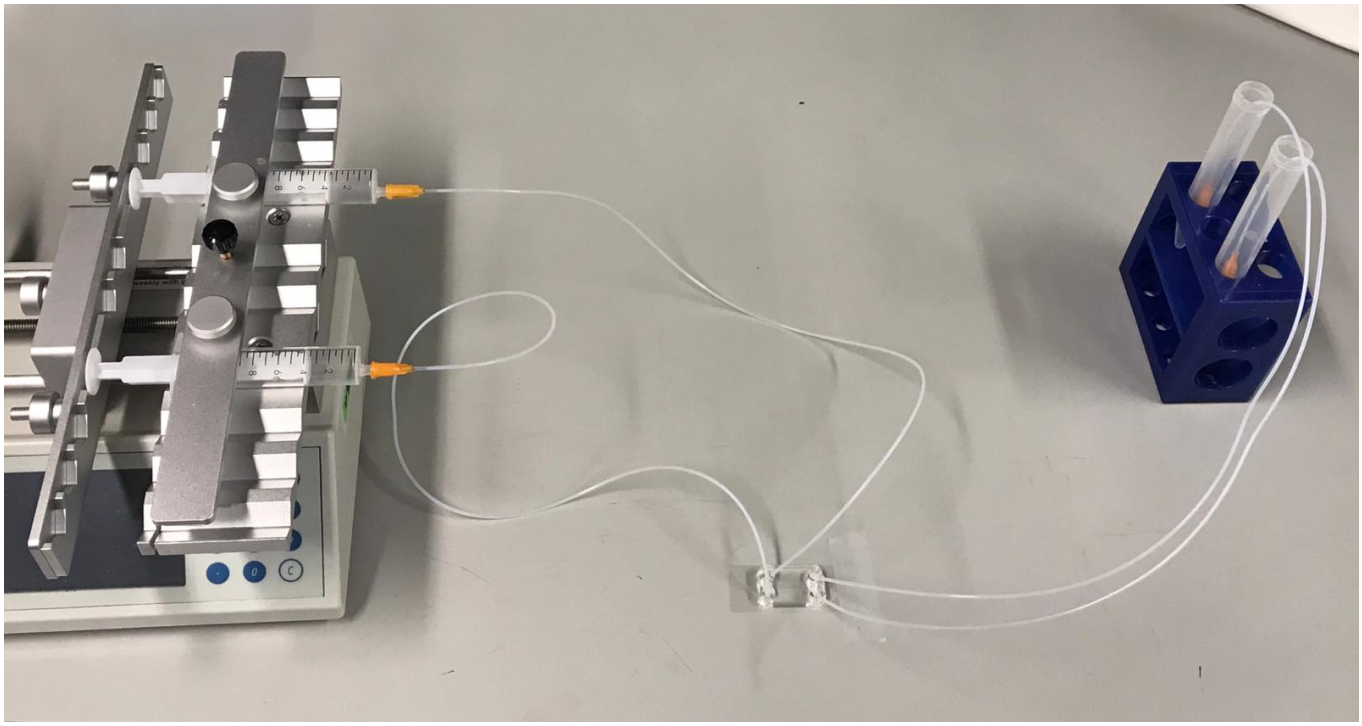

Figura 9: Experimental setup for the validation of the biomechanical model currently presented. Used and designed by Lopez A. [4]. From left to right, we see the syringes connected to the device, represented in Fig.8, and, on the right, the reservoirs for waste.

[1] Carmeliet P. Angiogenesis in life, disease and medicine. *Nature*, 438:932–936, 2005.

[2] Joel Linden. Adenosine in tissue protection and tissue regeneration. *Molecular Pharmacology*, 67(5):1385–1387, 2005.

[3] Folkman J. Transplacental carcinogenesis by stilbestrol. *New England Journal of Medicine*, 285(7):404–405, 1971.

[4] Lopez A., Castaño O., and Engel E. Design of a microphysiological system for angiogenesis assays to optimize the design of biomaterials (in progress). 2019.

[5] Ferrara N. and Kerbel R. S. Angiogenesis as a therapeutic target. *Nature*, 438:967–974, 2005.

[6] Hurwitz Herbert M.D. et al. Bevacizumab plus irinotecan, fluorouracil, and leucovorin for metastatic colorectal cancer. *New England Journal of Medicine*, 350(23):2335–2342, 2004.

[7] Guillermo Vilanova, Ignasi Colominas, and Hector Gomez. A mathematical model of tumour angiogenesis: growth, regression and regrowth. *Journal of The Royal Society Interface*, 14(126):20160918, 2017.

[8] Michael R. Mancuso et al. Rapid vascular regrowth in tumors after reversal of vegf inhibition. *The Journal of Clinical Investigation*, 116(10):2610–2621, 2006.

[9] Baffert et al. Cellular changes in normal blood capillaries undergoing regression after inhibition of vegf signaling. *American Journal of Physiology-Heart and Circulatory Physiology*, 290(2):H547–H559, 2006.

[10] Falcon et al. Reduced vegf production, angiogenesis, and vascular regrowth contribute to the antitumor properties of dual mtorc1/mtorc2 inhibitors. *Cancer Research*, 71 (5):1573–1583, 2011.

[11] Peirce S. M. Computational and mathematical modeling of angiogenesis. *Microcirculation*, 15(8):739–758, 2008.

[12] Megan M. Olsen and Hava T. Siegelmann. Multiscale agent-based model of tumor angiogenesis. *Procedia Computer Science*, 18:1016 – 1025, 2013.

[13] Amy L. et al. Bauer. A cell-based model exhibiting branching and anastomosis during tumor-induced angiogenesis. *Biophysical Journal*, 92:3105 – 3121, 2007.

[14] Katie Bentley, Holger Gerhardt, and Paul A. Bates. Agent-based simulation of notch-mediated tip cell selection in angiogenic sprout initialisation. *Journal of Theoretical Biology*, 250(1):25 – 36, 2008.

[15] M.A.J. Chaplain, S.R. McDougall, and A.R.A. Anderson. Mathematical modeling of tumor-induced angiogenesis. *Annual Review of Biomedical Engineering*, 8(1):233–257, 2006.

[16] Schugart R. C. et al. Wound angiogenesis as a function of tissue oxygen tension: A mathematical model. *Proceedings of the National Academy of Sciences*, 105(7):2628–2633, 2008.

[17] Mantzaris N. V., Webb S., and Othmer Hans G. Mathematical modeling of tumor-induced angiogenesis. *Journal of Mathematical Biology*, 49(2):111–187, 2004.

[18] K. J. Painter. Modelling cell migration strategies in the extracellular matrix. *Journal of Mathematical Biology*, 58(4):511, 2008.

[19] Travasso Rui D. M. et al. Tumor angiogenesis and vas-

cular patterning: A mathematical model. *PLoS ONE*, 6 (5):1–10, 2011.

[20] Guillermo Vilanova, Ignasi Colominas, and Hector Gomez. Capillary networks in tumor angiogenesis: From discrete endothelial cells to phase-field averaged descriptions via isogeometric analysis. *International Journal for Numerical Methods in Biomedical Engineering*, 29(10): 1015–1037, 2013.

[21] E. A. B. F. Lima, J. T. Oden, and R. C. Almeida. A hybrid ten-species phase-field model of tumor growth. *Mathematical Models and Methods in Applied Sciences*, 24(13):2569–2599, 2014.

[22] Miguel O. Bernabeu et al. Computer simulations reveal complex distribution of haemodynamic forces in a mouse retina model of angiogenesis. *Journal of The Royal Society Interface*, 11(99):20140543, 2014.

[23] Heike Emmerich. Advances of and by phase-field modelling in condensed-matter physics. *Advances in Physics*, 57(1):1–87, 2008.

[24] F. Campelo and A. Hernandez-Machado. Model for curvature-driven pearling inestability in membranes. *Physical review letters*, 99:088101, 09 2007.

[25] F. Campelo and A. Hernandez-Machado. Dynamic model and stationary shapes of fluid vesicles. *The European Physical Journal E*, 20(1):37–45, 2006.

[26] Nikolas Provatas and Ken Elder. *Phase-Field Methods in Materials Science and Engineering*. Wiley-VCH, 1st edition, 2010, pp. 39-48.